IAEA Technical Meeting on Plasma Disruptions and their Mitigation
July 20-23, 2020, WWW

Near-field models and simulation of the ablation of pellets and SPI fragments for plasma disruption mitigation in tokamaks

Roman Samulyak, James Yuan, Nizar Naitlho, Nicholas Bosviel
Stony Brook University

Paul Parks, *General Atomics*

Work supported by SciDAC ***Center for Tokamak Transient Simulations***

Introduction: near-field models and codes for pellet ablation

Local Model

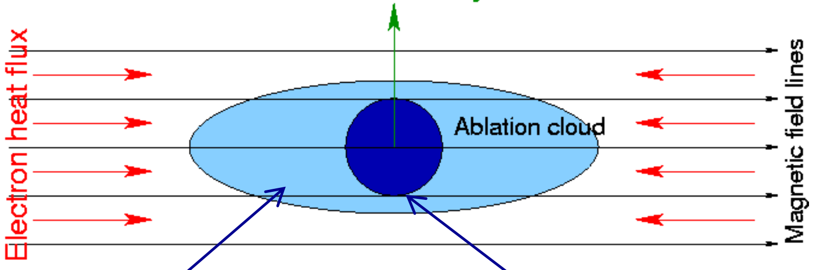

- Phase transition (ablation model) for pellet surface

- Kinetic model for the electron heating
- Low magnetic Re MHD equations
- EOS with atomic processes, radiation
- Grad B drift models for ablated material
- Pellet cloud charging models

Local Codes

FronTier (FT)

- Hybrid Lagrangian-Eulerian code with explicit interface tracking
- Both pellet surface and ablation cloud – plasma interface are explicitly tracked
- 2D axisymmetric simulation of the ablation of single neon or deuterium pellets, computing ablation rates

FT simulation of neon pellet in 2T magnetic field

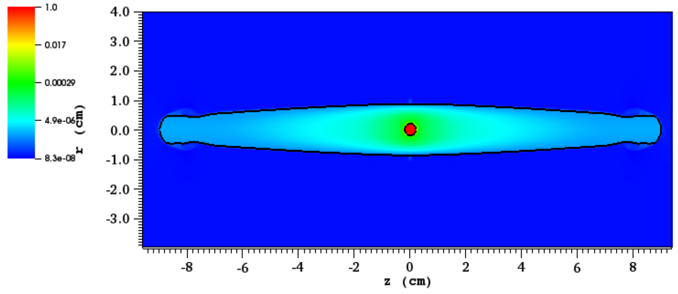

Lagrangian Particle code (LP)

- Highly adaptive 3D particle code, massively parallel
- Lagrangian treatment of ablation material eliminated numerous numerical difficulties associated with ambient plasma, fast time scales etc.
- Supports many SPI fragments in 3D
- R. Samulyak, X. Wang, H.-S. Chen, J. Comput. Phys., 362 (2018), 1-19.

LP simulation of neon pellet in 2T magnetic field with grad B drift (left) and SPI fragments (right)

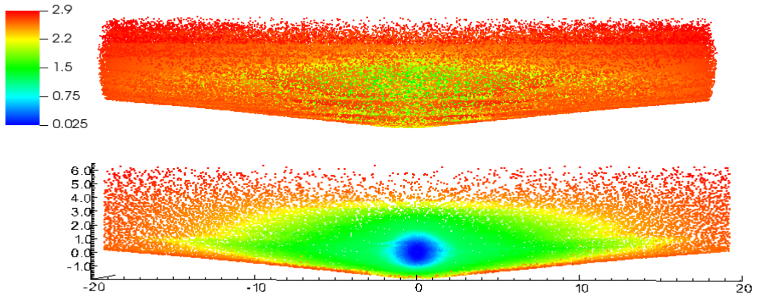

Main physics models and governing equations: MHD equations in Low Magnetic Reynolds Number Approximation

The ablation cloud expansion is governed by the inviscid, compressible Euler's equations with electromagnetic terms:

$$\frac{\partial \rho}{\partial t} = -\nabla \cdot (\rho \boldsymbol{u}),$$

$$\rho \left(\frac{\partial}{\partial t} + \boldsymbol{u} \cdot \nabla \right) \boldsymbol{u} = -\nabla P + \boldsymbol{J} \times \boldsymbol{B},$$

$$\rho \left(\frac{\partial}{\partial t} + \boldsymbol{u} \cdot \nabla \right) e = -P \nabla \cdot \boldsymbol{u} + \frac{1}{\sigma} \boldsymbol{J}^2 - \nabla \cdot \boldsymbol{q},$$

$$P = P(\rho, e).$$

$\boldsymbol{J} = \sigma(-\nabla\varphi + \boldsymbol{u} \times \boldsymbol{B})$

$\nabla\, \sigma\, \nabla\varphi = \nabla \cdot (\boldsymbol{u} \times \boldsymbol{B}),$

subject to boundary conditions

We assume that the potential is constant in the pellet ablation cloud, and

$$J_\theta = \sigma_\perp u_r B$$

Physics models: Electron Heat Flux

Parks heat flux model (2019):

$$-\nabla . q = \frac{q_\infty n_e(r,z)}{\tau_{eff}} [g(u_+) + g(u_-)]$$

where,

$$g(u) = u^{1/2} K_1(u^{1/2})/4,$$

$$u_\pm = \frac{\tau_\pm}{\tau_{eff}},$$

$$\tau(r,z) = \int_\infty^z n_e(r,z')\, dz',$$

$$\tau_{eff} = \tau_\infty \frac{1}{0.625+0.55\sqrt{1+Z_*}},$$

$$\tau_\infty = \frac{T_{e\infty}^2}{8\pi e^4 ln\lambda}$$

Transverse Conductivity

Transverse electric conductivity (Parks, 2017):

$$\sigma_\perp = \frac{9700T^{3/2}}{Zln\lambda + 0.00443T^{2.245}\frac{n^0}{n_e}}$$

In the absence of neutrals,

$$\sigma_\perp \rightarrow \sigma_\perp^s = \frac{9700T^{3/2}}{Zln\lambda}$$

From the tabulated EOS derived from solving the Saha system, the fraction $\frac{n^0}{n_e}$ is readily available in the code via quick look ups.

Equation of State with Saha LTE ionization model. Radiation model.

The system is closed using either the ideal gas EOS (for benchmarking and verification) or a tabulated EOS generated from solving the Saha equations :

$$\frac{f_{m+1} f_e}{f_m} = \frac{2m}{\rho} \frac{u_{m+1}}{u_m} \left(\frac{2\pi m_e kT}{h^2} \right)^{3/2} \exp\left(-\frac{I_{m+1}}{kT} \right), \quad m = 1, \ldots, Z,$$

along with conservation conditions: $\sum_m f_m = 1\,, \; \sum_m m f_m = f_e$

Finally,

$$P = (1 + f_e) \frac{\rho kT}{m_a}$$

$$e = \frac{3}{2} (1 + f_e) \frac{kT}{m_a} + \frac{1}{m_a} \sum Q_m f_m + \frac{1}{m_a} \sum W_m f_m$$

- Fully coupled system of nonlinear equations; difficult to solve in each point at each time step of a hydro code
- Both FronTier and Lagrangian Particle codes use tabulated data sets pre-computed by Saha equation solver
- **Non-LTE radiation in thin optical limit** using data sets pre-computed by CRETIN code

Boundary Conditions at the Pellet Surface

- Heat conduction in the pellet can be neglected: the diffusion of heat is slower compared to the removal of pellet material by ablation
  - The surface temperature remains constant

- Heat flux at the surface:

$$q_{\pm} = \frac{1}{2}\, u_{\pm} K_2(u_{\pm}^{1/2})$$

- This heat flux is completely used for phase transition, defining the mass flux:

$$\frac{q_{\pm}}{\varepsilon_s} = \rho v_n$$

- The backward characteristic from the cloud to the pellet surface:

$$\frac{dv_n}{d\lambda_-} - \frac{1}{\rho c}\frac{dP}{d\lambda_-} = \Gamma \frac{\partial q}{\partial z}\,, \text{ where } \frac{d}{d\lambda_{\pm}} = \frac{\partial}{\partial t} + (v_n \pm c)\frac{\partial}{\partial n}$$

- These equations give a closed system. We solve it to find thermodynamic states and velocity at the pellet surface

Grad-B Drift Model for Lagrangian Particle Code

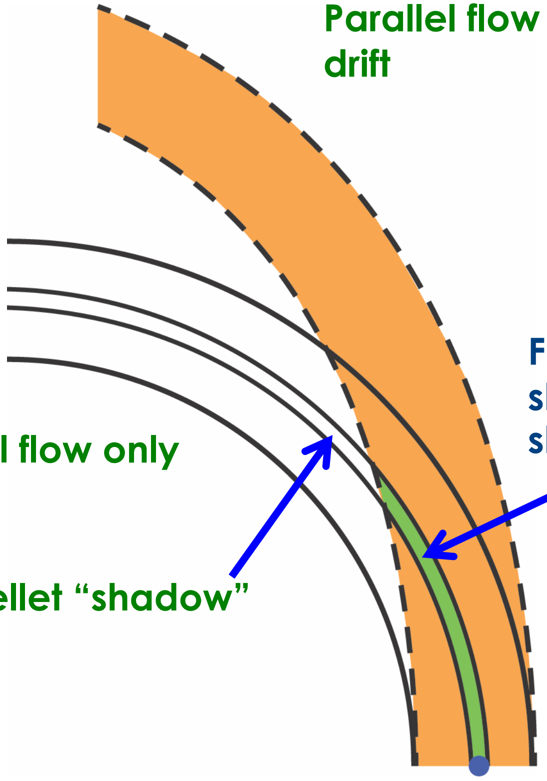

Grad-B drift model:

- We assume that the electrostatic potential is always uniform along the magnetic field. The equation for the horizontal grad-B drift velocity in the x (large-R) direction is governed by the formula [Rozhansky 1995, 2004, Parks and Baylor, 2005]

$$\frac{dv_D}{dt} = \frac{2}{R\langle\rho\rangle}\left\langle P\left(1+\frac{M^2}{2}\right) - P_\infty\right\rangle$$

where $\langle A\rangle \equiv \int_0^\infty A\,dz$, and *R* is the tokamak major radius

- Integrations are evaluated in the LP code with the kinetic heating algorithms
- Typical major radii of 1.6 m (DIII-D) and 6.2 m (ITER) are used in simulations

Simulation results
I. Verification and Code Comparison

- Both FronTier and Lagrangian particle code are in good agreement with theory (improved NGS model) for spherically symmetric simulations
- Simulations in a wide range of plasma temperatures and pellet radii confirmed theoretical scaling laws
- While FronTier computes spherically symmetric problems in 1D, the Lagrangian particle code performs simulations in 3D with symmetric initial conditions (LP errors are of the order of 1%)

Te = 2 keV

r_p(cm)	Theory	FronTier 1/27/20	% error
0.1	25.5245	25.60	+0.296
0.2	64.9295	64.53	-0.615
0.5	222.206	220.9	-0.588
0.7	348.814	347.3	-0.434

Te = 5 keV

r_p(cm)	Theory	FronTier 1/27/20	% error
0.1	25.5245	25.60	+0.296
0.2	64.9295	64.53	-0.615
0.5	222.206	220.9	-0.588
0.7	348.814	347.3	-0.434

Te = 8 keV

r_p(cm)	Theory	FronTier 1/27/20	% error
0.1	116.815	117.0	+0.158
0.2	297.469	295.4	-0.695
0.5	1019.02	1013	-0.589
0.7	1600.07	1591	-0.567

MHD simulations with fixed shielding length of the ablation cloud

- As the ablation material heats up and ionizes, it propagates along magnetic field lines, increasing the pellet shielding. Grad-B drift of the ablated material across magnetic field lines established finite shielding length for the pellet
- The axisymmetric pellet ablation code FronTier cannot resolve the grad-B drift effect
- A fixed shielding length was imposed in FronTier, theoretically estimated as 16 cm
- For the purpose of code comparison and verification, the grad-B effect in the Lagrangian particle code was turned off and the fixed 16 cm shielding half-length was imposed
- Both code achieve good agreements on the reduction of ablation rates in magnetic fields

- The following canonical parameters were used in simulations
  - r_p = 2 mm
  - T_e = 2 keV
  - $n_e = 10^{14}$ 1/cc with electrostatic shielding = 1.205×10^{13} for neon and
    = 1.38×10^{13} for deuterium

Reduction of the ablation rate in magnetic field

Neon pellets

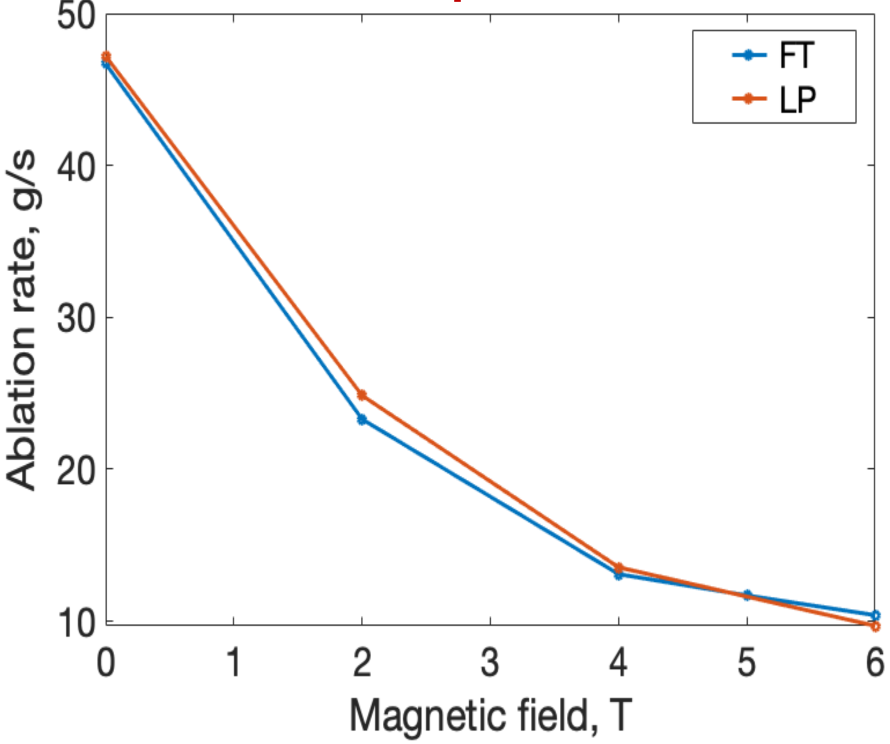

B, T	G (FT, g/s)	G(LP, g/s)
2	24.86	23.3
4	13.55	13.1
5		11.7
6	9.7	10.4

Deuterium fueling pellets

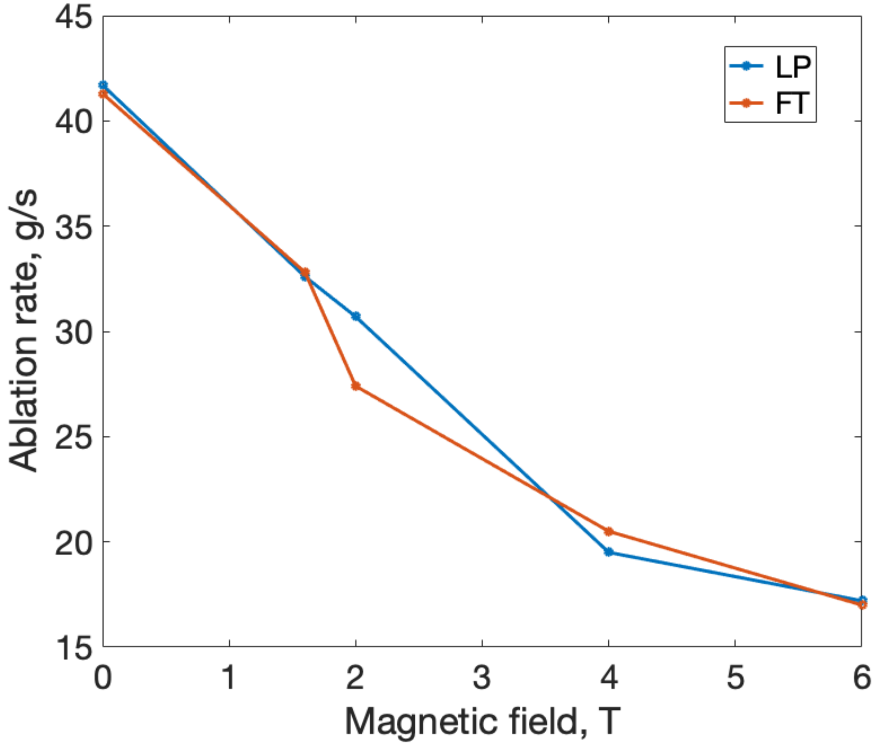

B, T	G (FT, g/s)	G(LP, g/s)
1.6	32.8	32.6
2	27.4	30.7
4	20.5	19.5
6	17	17.2

- Ionized ablation flow moves predominantly along magnetic field lines; density and pellet shielding increases
- Higher magnetic fields lead to narrower pellet clouds, higher densities and lower ablation rates. Significant reduction of the ablation rate was observed
- Both codes are in very good agreement on the reduction of ablation rates

MHD simulations of neon and deuterium pellets with grad-B drift

- Simulations were performed with the Lagrangian particle code
- The shielding length was obtained self-consistently
- The following canonical parameters were used in simulations
  - $r_p = 2$ mm
  - $T_e = 2$ keV
  - $n_e = 10^{14}$ 1/cc with electrostatic shielding = 1.205×10^{13} for neon and
    = 1.38×10^{13} for deuterium
  - Tokamak major radius R = 1.6 m for DIII-D and R = 6.2 m for ITER

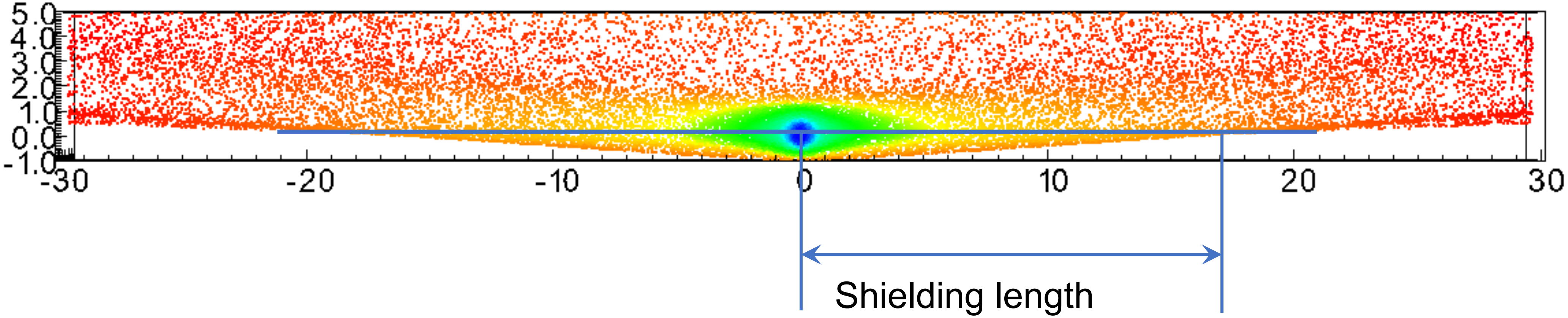

Reduction of the ablation rate in magnetic field for neon pellets: fixed shielding length compared to self-consistent shielding length

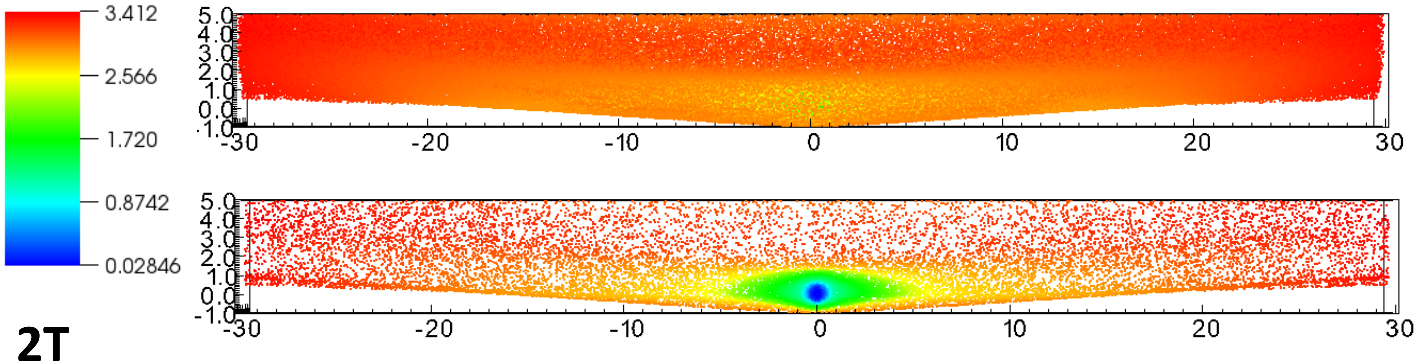

2T

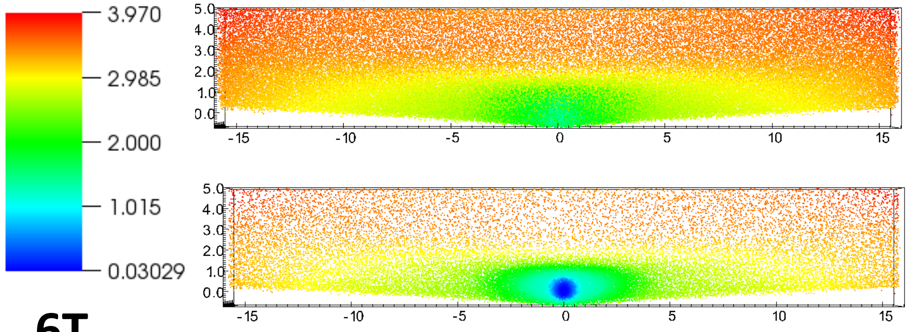

6T

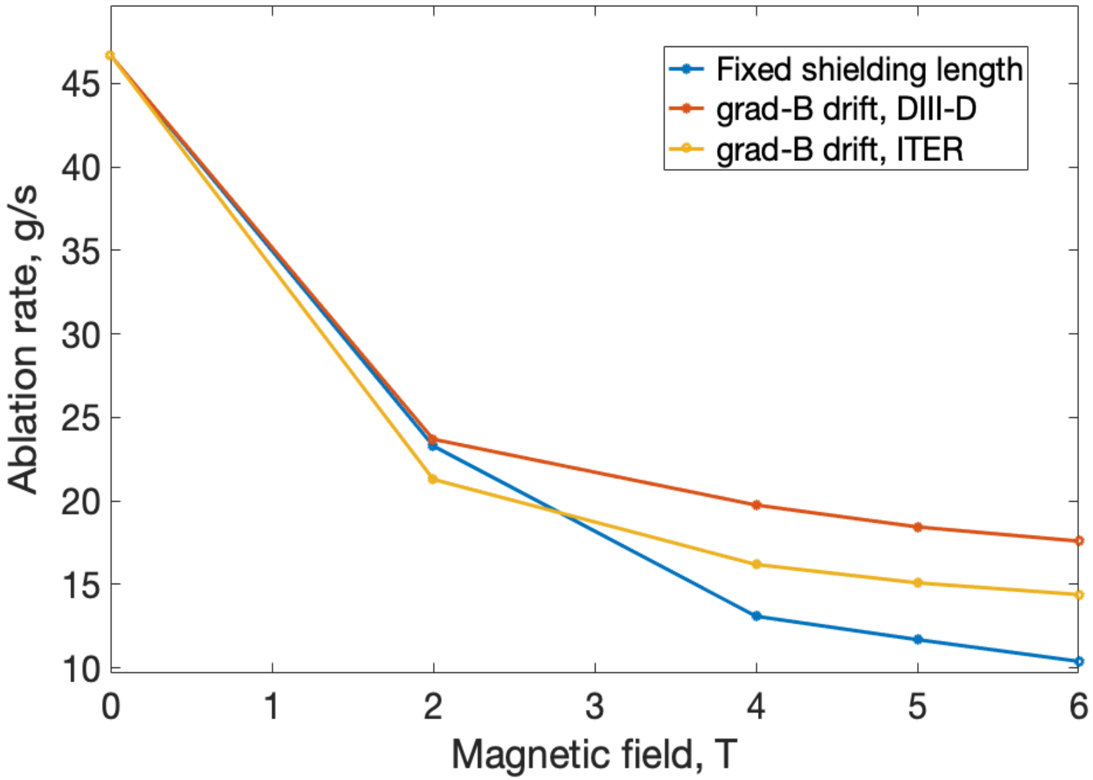

B (T) DIII-D	Shielding length, cm	G(LP, g/s)
2	18	23.7
4	14	19.76
5	13	18.45
6	12	17.6

B (T) ITER	Shielding length, cm	G(LP, g/s)
2	35.5	21.3
4	30	16.2
5	27.5	15.1
6	25.5	14.4

Weaker reduction of the ablation rate in magnetic field in simulations with grad-B drift compared to simulations with fixed shielding length. Grad-B drift effect in DIII-D is stronger compared to ITER.

Reduction of the ablation rate in magnetic field for deuterium fueling pellets: fixed shielding length compared to self-consistent shielding length

B (T) DIII-D	Shielding length	G(LP, g/s)
1.6	30 cm	35.2
2	27 cm	33.4
4	17 cm	29.7
6	15 cm	27.5

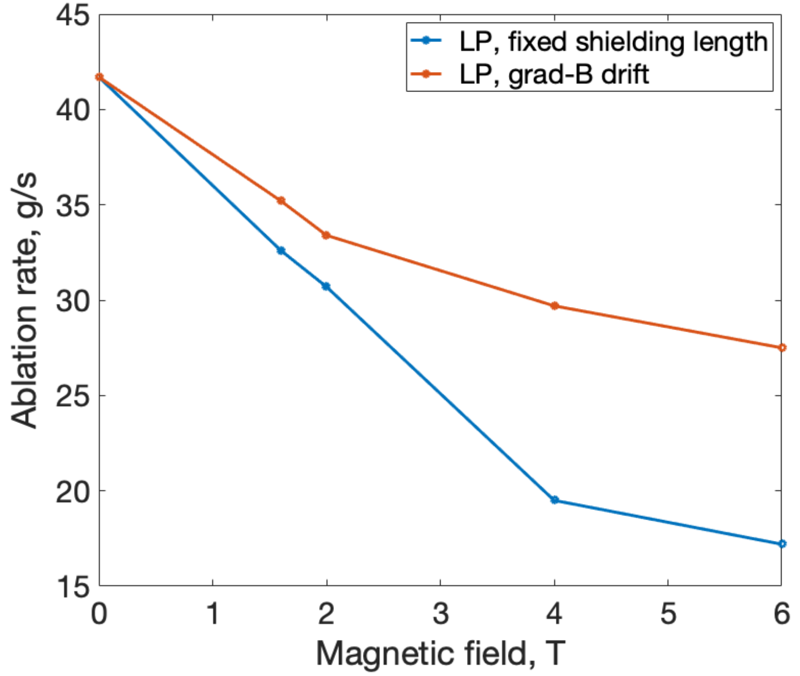

- With grad-B drift, we observe weaker reduction of the ablation rate in magnetic field compared to simulations with fixed shielding length
  - This is due to a combine effect of shorter shielding lengths and slightly changed hydrodynamic states in the ablation cloud
  - Grad-B drift in DIII-D (R_0 = 1.6 m) is stronger compared to ITER (R_0 = 6.2 m), all other factors assumed equal
  - The ablation rate of 35.2 is within 10% of the experimentally measured value (39 g/s)

- Any empirical G(B) fitting functions should be aware of the tokamak major radius
- Since B/R does not change significantly for various tokamaks (B/R ~ 1), we are building a pellet ablation database assuming constant B/R ratio

Dependence of ablation rates on magnetic field in the presence of grad B drift

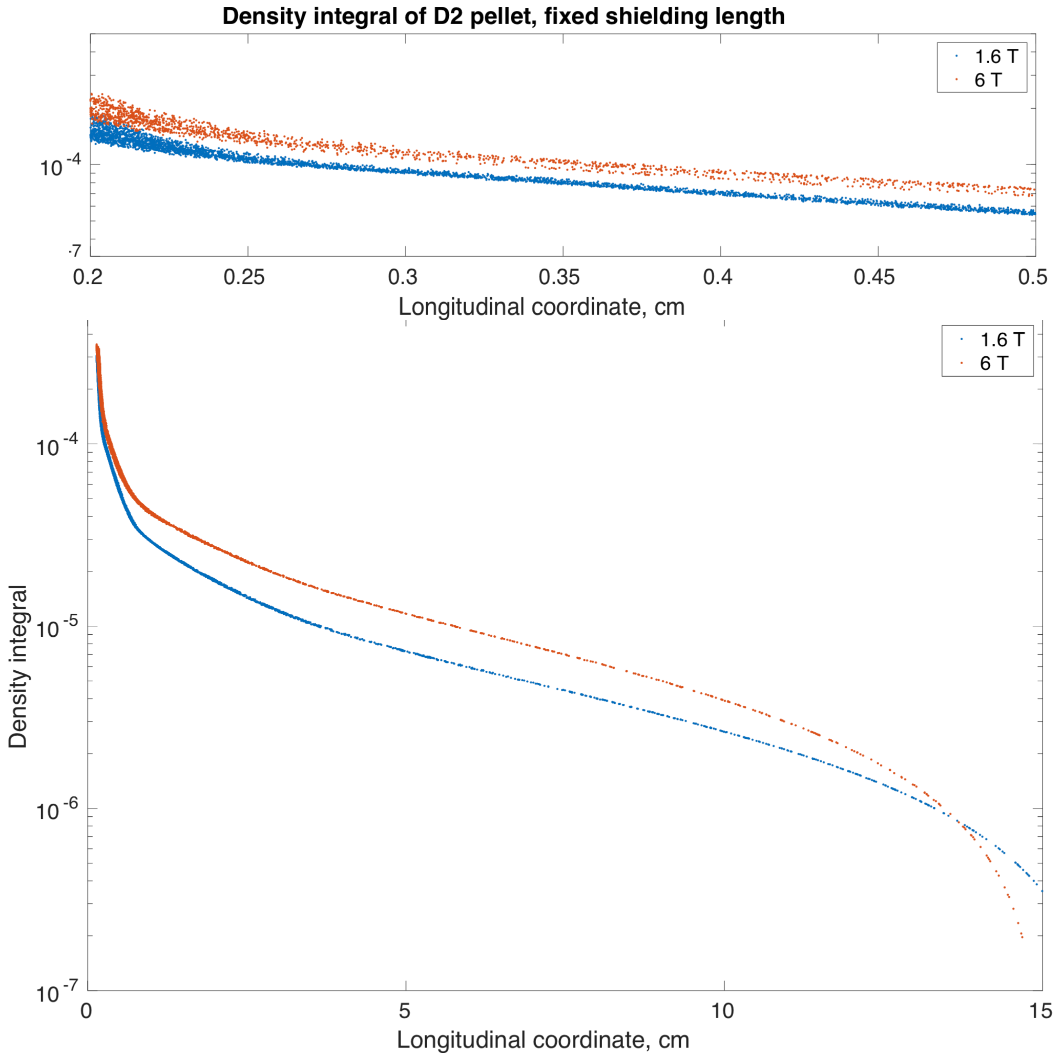

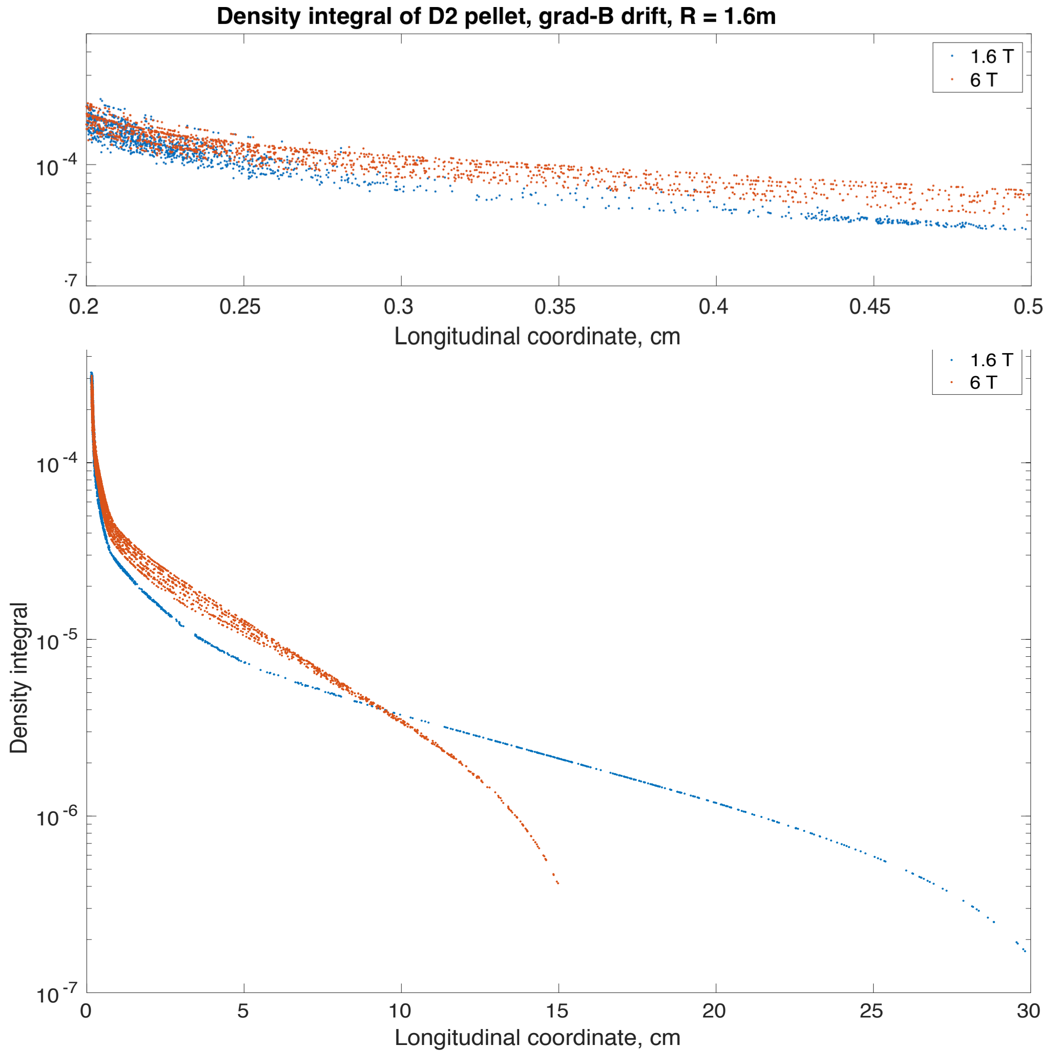

- Top images: behavior of the density integral near the pellet surface. Bottom images: its behavior in the whole domain
- With fixed shielding length, the density integral (that defines attenuation of the incoming electron heat flux) is higher for 6T field compared to 1.6 T
- With grad-B drift, both density integrals are close near the pellet surface

Influence of radiation model

- All simulation results for neon pellets presented above used a thin optical limit radiation model and a database precomputed with the CRETIN code
- Additional analysis shows that re-absorption of radiation could be important

- Using the PrismSPECT code, E. Hollmann and P. Parks computed an emissivity table by considering the full neon radiation spectrum and the radiation absorption in a density – temperature thermodynamic domain typical for neon pellet ablation clouds

- Simulations with such a reduced radiation model resulted in significantly increased temperatures. In turn, the increased temperature caused more intense radiation

- Full radiation model had a small effect on the pellet ablation rates. As expected, the ablation rates increased. For the 2 mm neon pellet in 2T magnetic field, the ablation rates are:
  - Thin optical limit radiation model: G = 23.3 g/s
  - PrismSPECT-based radiation model: G = 27 g/s for the case of fixed 16 cm shielding length and
G = 30 g/s for simulation with grad-B drift (18 cm shielding length)

- On the next two slides, we present comparison of some relevant propertied of the ablation cloud for 2 mm neon pellet ablation in 2 T field using 16 cm shielding length
  - Label “Old model” stands for the thin optical limit radiation model
  - Label “New model” stands for the radiation model based on the emissivity table from PrismSPECT

Comparison of radiation and electron heat power densities in two radiation models

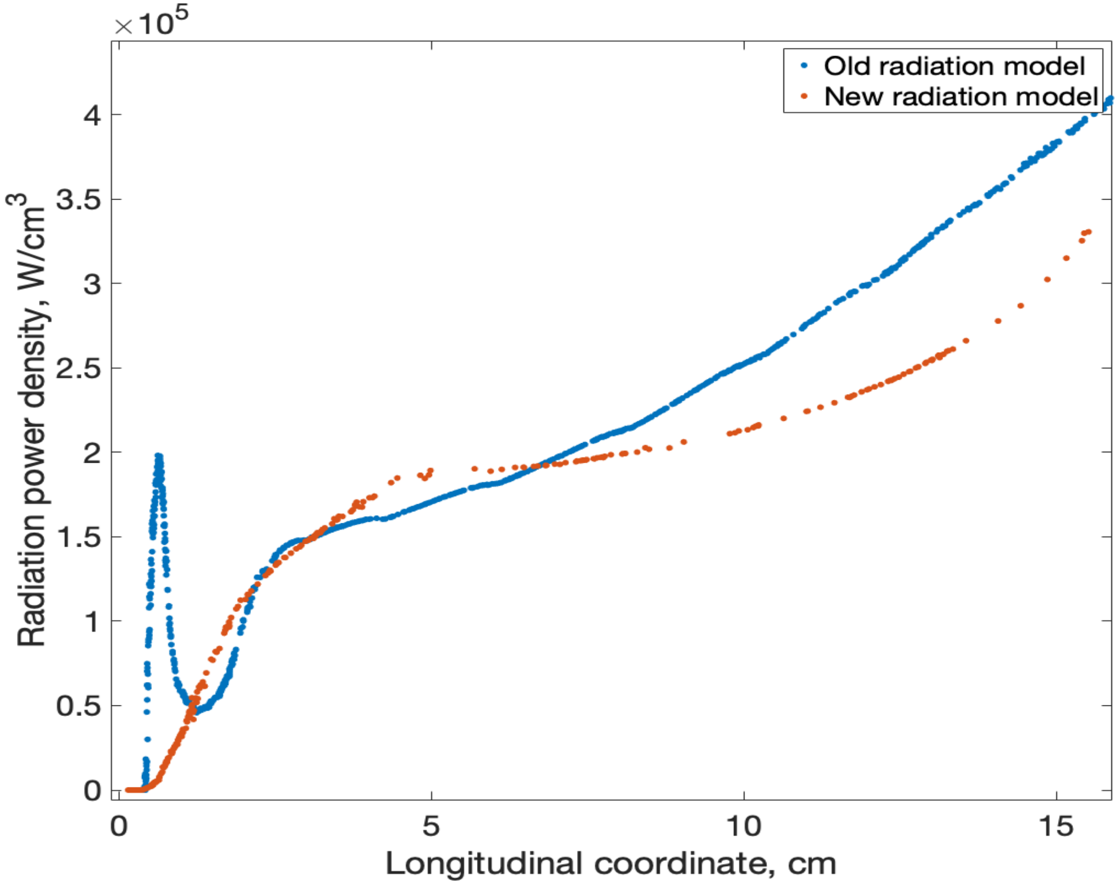

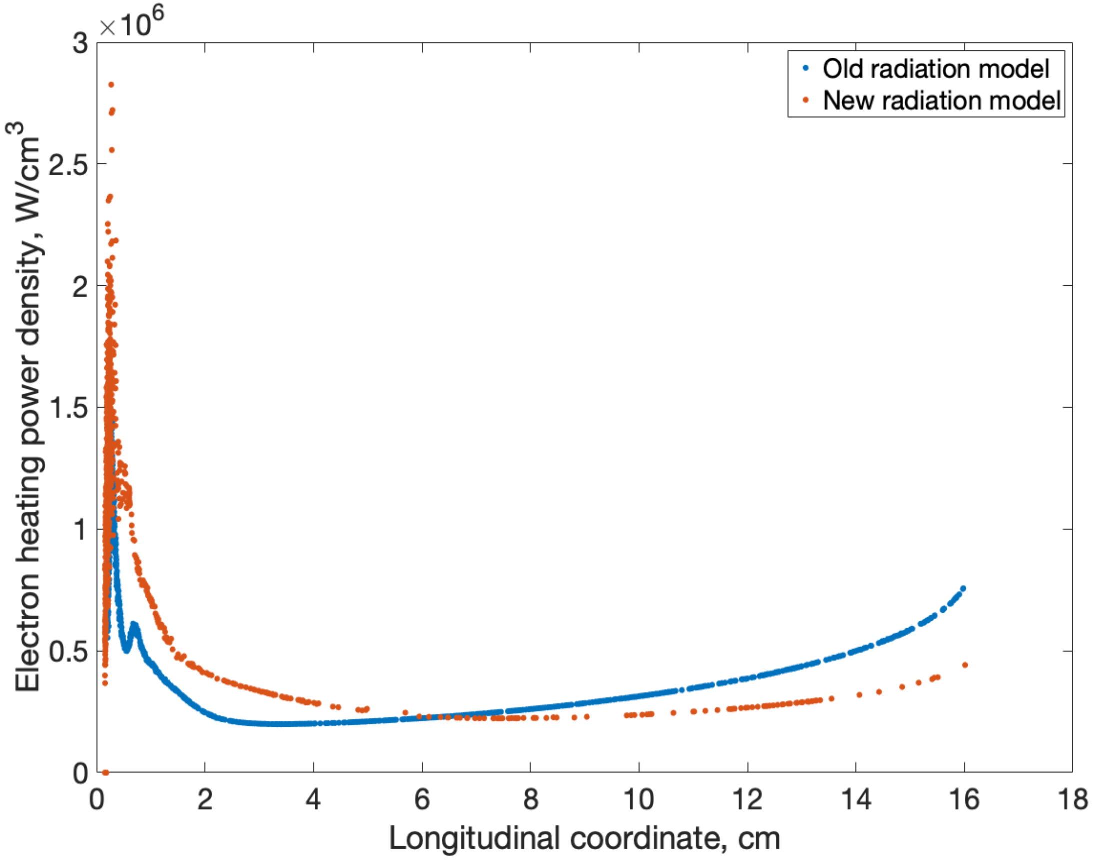

- The new radiation model predicts lower radiation power (left plot) close to the pellet surface (1-3 cm) due to re-absorption, as well as in the far field (7 – 16 cm)

- The new radiation model predicts slightly higher electron heat power density closer to the pellet surface (right plot)
- Due to lower radiation with the new radiation model in the far field, the temperature increases causing higher pressure and velocity, and lower density. Because of lower densities in the cloud, the electron heat deposition is smaller compared to the old model.

Ratio of electron heat and radiation power densities in two radiation models

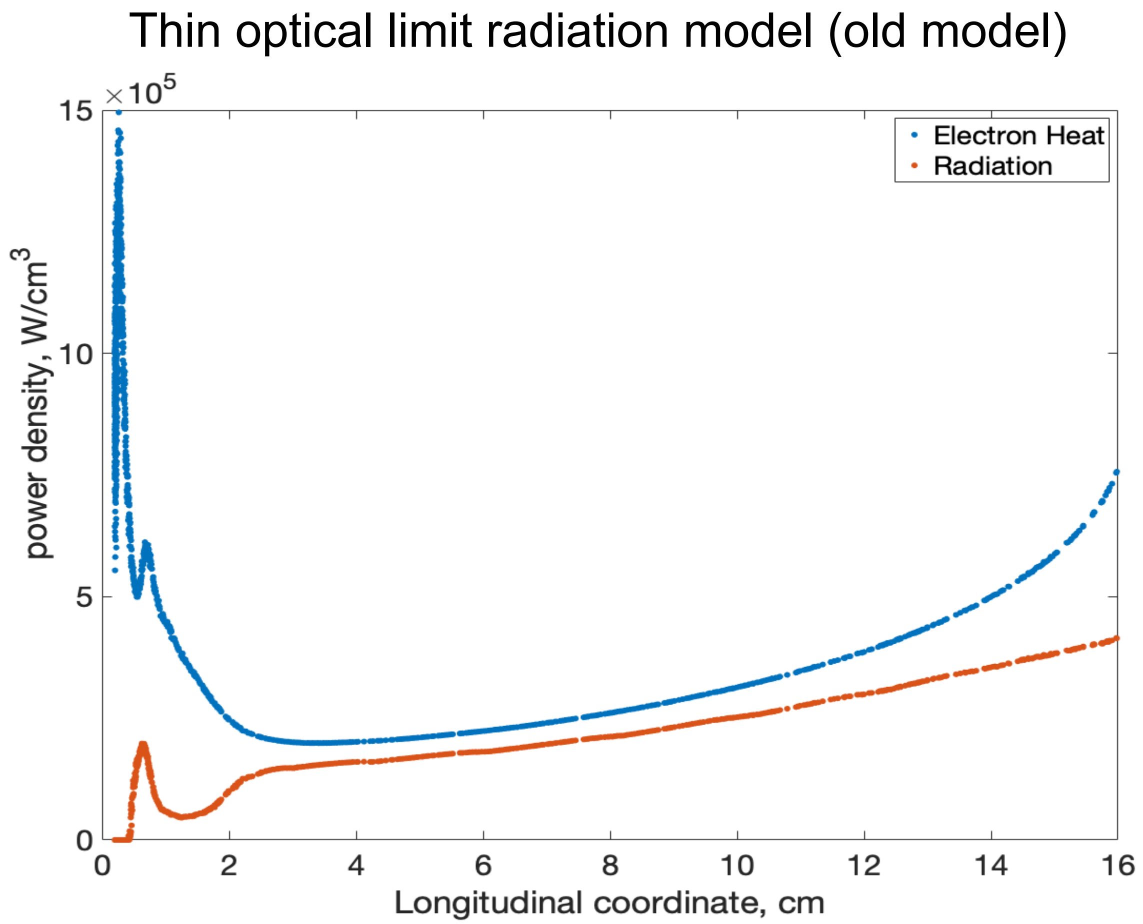

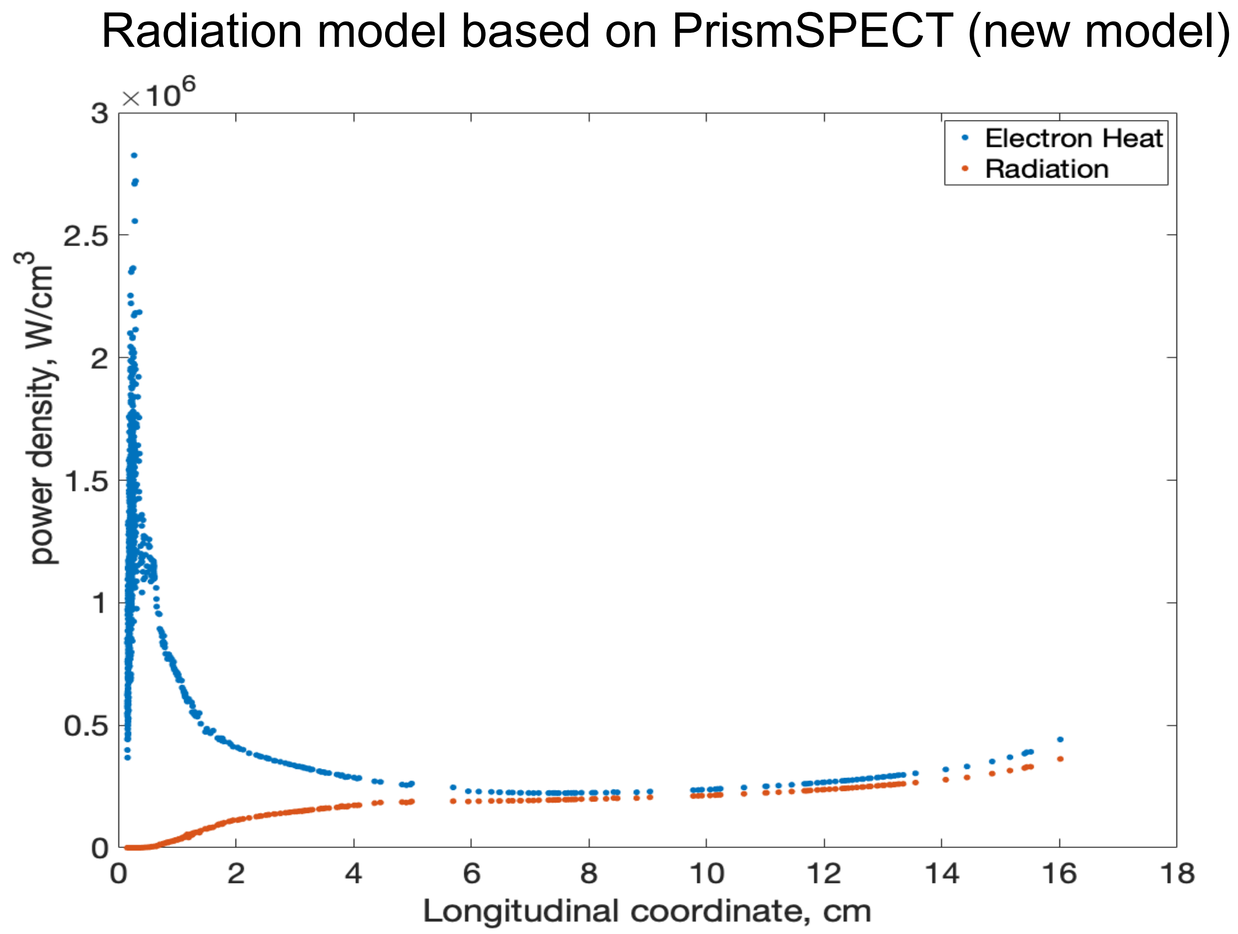

- With both radiation models, the electron heat flux is significantly higher than radiation close to the pellet surface
- With the new radiation model, radiation is much close to the electron heat flux in the far field
- The increase of the ablation rate with the new radiation model is quite small

Work in progress: simulation of SPI

Initial setup

Experimental image of the barrel with neon pellet fragments (Baylor, 2018) is shown

- For DIII-D, the total neon inventory is N_0 = 0.0213 moles
- This amount is contained in in a large pellet with r_{big} = *0.41 cm* (*W* = 20.183 amu is the atomic mass of neon and ρ = 1.444 g/cc is the mass density of frozen neon)
- The pellet is expected to shatter into *N* = 250 smaller fragments. Therefore, the average radius of a spherical fragment is $r_{fragment}$ = 0.66 mm
- Assuming a uniform distribution of fragments throughout the cluster stream whose diameter is chosen as d = 30 cm, length L = 30 cm (with the volume of V = 21206 cc), we obtain the distance between fragments as ~4.4 cm

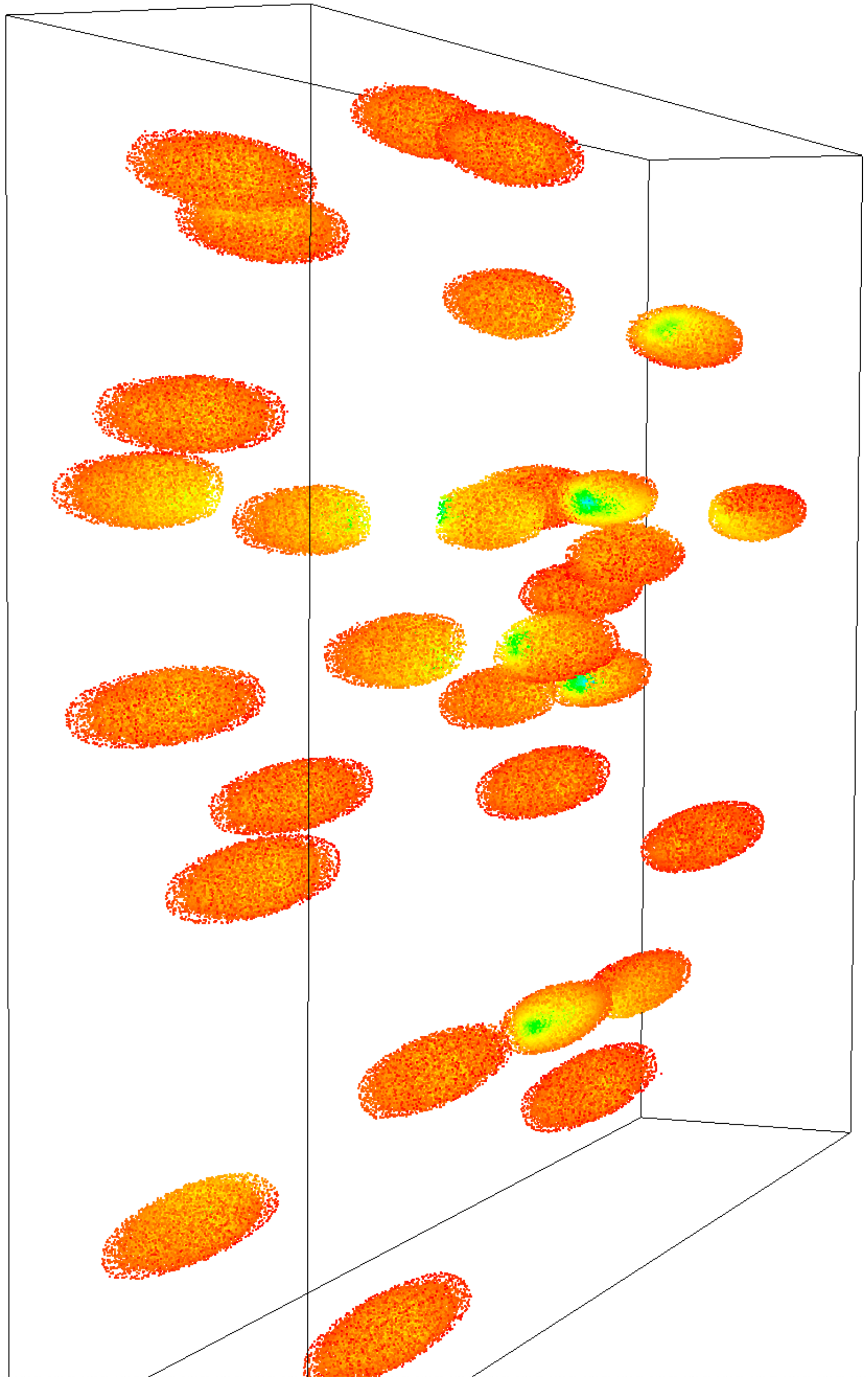

Work in progress: simulation of SPI

- Current simulations operate with a slice of the pellet fragment plume with fully resolved size in the directions of the magnetic field and the direction of grad-B drift. The slice is approximately 5 cm thick in the transverse direction.
- The slice contains approximately 40 fragments distributed randomly

- The following cooling model for the ambient plasma is applied

$$\frac{d}{dt}\left(\frac{T}{T_0}\right)^{5/4} = -\frac{N}{N_{max}}\frac{1}{t_{cool}}$$

where T_0 = 2000 eV, T is current plasma temperature, N_{max} is the total number of neon atoms in SPI fragments, N is the averaged number of ablated neon atoms, and t_{cool} is the cooling time (need to discuss some details as this will affect the spatial distribution of plasma cooling; implementation of cooling could be done similarly to density integrals for the kinetic models)

- For the given conditions, N_{max} = 1.28e22 and t_{cool}= 38.5 microseconds

- Simulations of small number of fragments have been completed

Current work (in collaboration with N. Ferraro (PPPL), B. Lyons, C. Kim, L. Lao (GA))

Multiscale coupling of Lagrangian particle pellet ablation code with NIMROD / M3D-C1

NIMROD simulation domain showing ablated material obtained from LP code

LP simulation of pellet ablation cloud

B, n_e, T_e from TK to LP

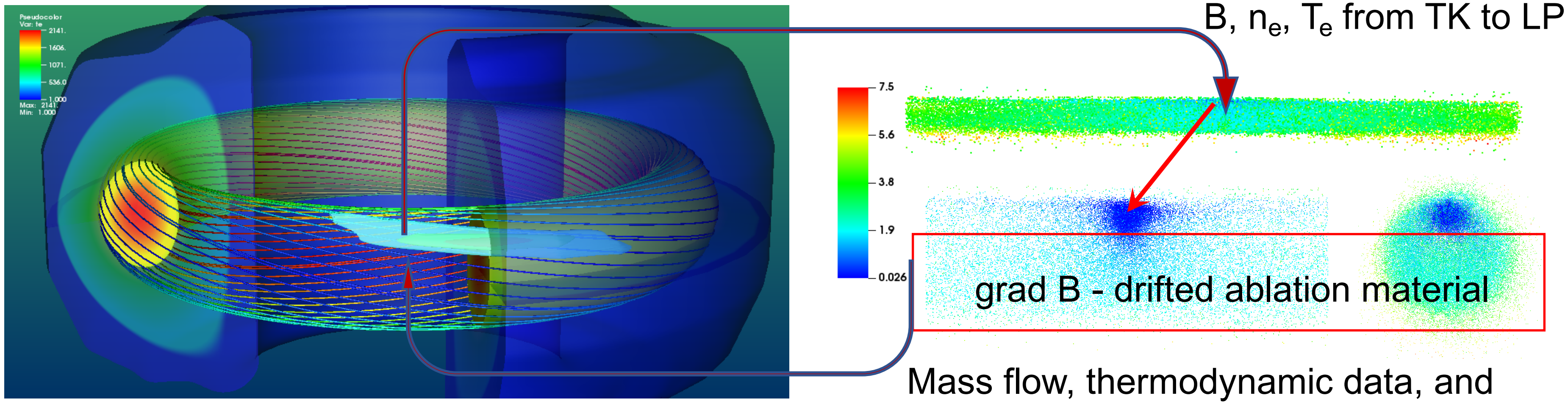

Mass flow, thermodynamic data, and energy sinks from LP to TK

Schematic of multiscale coupling

- **Grad B drift provides physics-based separation of scales for coupling**
- LP code evolves self-consistently the entire ablation cloud that provides pellet shielding
- grad B drift model in the LP code propagates ablated material across magnetic field lines, establishing the cloud shielding length. Ablated material that drifted beyond the main ablation cloud is transferred to the tokamak code, together with thermodynamic data and energy sinks. Particle representation ensures conservative mass transfer
- LP code obtains the magnetic field and electron density and temperature from the tokamak code

- LP data input has been successfully incorporated in NIMROD
- A virtual code camp has been scheduled August 3-6 that will involve General Atomics, PPPL and SBU scientists and PhD students. We expect to complete multiscale coupling and obtain fully operating code

Summary and Conclusions

- Simulation of neon and deuterium pellets with the resolution of all relevant physics models have been performed using the interface tracking FronTier code (2D axisymmetric), and the 3D Lagrangian particle code with high level of numerical adaptivity
    - A rigorous verification program gas been completed. Both codes are in good agreement with the improved NGS model for spherically-symmetric simulations
    - Both codes agree on the reduction of pellet ablation rates in magnetic field

- Using Lagrangian particle (LP) code, MHD simulations with grad-B drift have been performed
    - Magnetic field reduction of ablation rates is smaller compared to simulations with fixed shielding length
    - LP results on deuterium pellets are within 10% of the experimental values
    - Investigated a radiation model for neon that accounts for partial reabsorption of radiation. The corresponding ablation rates slightly increase

- Started full 3D simulations of SPI (simulations of small number of fragments have been completed)

- Developed a multiscale coupling method of with M3D-C1 and NIMROD
    - Well-defined, physics-based separation of scales
    - LP data input has been successfully incorporated in tokamak codes; work is expected to be completed during the code camp in August

- Future work:
    - Continue V&V; perform runs with fully coupled codes
    - New physics: DT / neon mixtures, kinetic heating by runaway electrons